2002

Non-Dimensional Parameter Development For Transcritical Cycles

H. E. Howard
Praxair

Non-Dimensional Parameter Development for Transcritical Cycles

Henry Howard, Sr. Development Associate, Praxair, Inc. 175 East Park Drive, P.O. Box 44
Tonawanda, NY 14150-7891, USA; Tel.: 716/879-2764; Fax: 716/879-7567
E-Mail: hank_howard@praxair.com

ABSTRACT

Increased commercial interest with regard to carbon dioxide's use in transcritical cycles has led to numerous modifications to the basic vapor compression cycle. The transcritical refrigeration cycle is characterized by the fact that supercritical high-side pressure is an optimization variable. Most cycle adaptations have been conceived with the intent of facilitating optimal high side pressure control. Depending upon operating range, improper high-side pressure definition may lead to power penalties in excess of 10%. A critical element in system design and optimization involves the mechanism for dynamic computation of the optimal high side pressure. Common approaches to this problem involve heuristics and empirical correlation. Unfortunately, such approaches are not phenomena-based. Application of such techniques limits the flexibility afforded to the control system.

The approach introduced relies upon fundamental thermodynamic considerations. Optimal high side pressure is analyzed through consideration of real gas properties. These evaluations have resulted in the identification of key non-dimensional parameters that drive high-side pressure optimization. A combination of non-dimensional parameters and selected system observations form an effective computational mechanism suitable for process control. A database of thermodynamic properties for CO_2 confirms the subject model's integrity and utility. Accuracy comparable to empirical models is achievable with far less complexity. The fundamental nature of the model allows for a common optimization means independent of operating specification and working fluid.

NOMENCLATURE

a: compressor performance correlation coefficient(s)
A: Ratio of compressor performance coefficients
b: Adiabatic compression power constant
C: Mass Heat Capacity
COP: Coefficient of Performance
f: 1/COP
h: Enthalpy
k: Heat Capacity Ratio, C_p/C_v
m: Mass Flow
P: Pressure
Q: Energy Flow
R: Ideal Gas Constant
T: Temperature
x: Mass Fraction Liquid
y: Non-dimensional, P_r^{γ}
Z: Compressibility

Greek Symbols
β: Compressor energy-flow parameter
γ: Adiabatic compression power, (k-1)/k
ΔH_{lv}: Latent heat of vaporization
η: Adiabatic compressor efficiency
Θ: Non-dimensional parameter, $\Phi+\Psi$
Φ: Non-dimensional parameter
Ψ: Non-dimensional parameter

Subscripts
h: high-pressure side
l: low-pressure side
p: constant pressure
r: ratio
v: constant volume
evap: evaporator
comp: compressor
gc: gas cooler

Subscripts consistent with Figure 1
1: Compressor Outlet
2: Gas Cooler Outlet
3: High Pressure SLHX outlet
4: JT Valve Outlet
5: Evaporator Outlet
6: Low Pressure SLHX outlet

Superscripts
ig: Ideal gas
r: Residual property

INTRODUCTION

Growing concern over hydrofluorocarbon contributions to global warming has led to consideration of alternative, natural refrigerants[1]. Among natural working fluids, CO_2 represents a fluid of particular interest because of low toxicity, cost, availability and thermophysical properties. CO_2 applications of particular commercial significance include automotive air conditioning, residential water heat pumps and cascade refrigeration systems.

By definition, a transcritical cycle possesses a gas cooler and evaporator operating above and below the critical pressure, respectively. Effective gas cooler operation at supercritical pressures results in a control problem foreign to common vapor compression cycles. Compressor discharge pressure is no longer defined by conditions of saturation within the condenser. In contrast, the transcritical cycle should be optimized with respect to compressor discharge pressure. As a consequence, the minimization of cycle power requires a control strategy incorporating dynamic optimization. Many physical modifications to the transcritical vapor compression cycle have been proposed with the intent of facilitating optimal high side pressure control[2,3].

Previous approaches to this problem have centered upon empirical correlation[4] and/or control heuristics[5]. Past thermodynamic considerations[6] have suffered from a failure to tie system observations to the characteristics associated with optimal high side pressure. The primary deficiencies associated with previous effort are a result of model inflexibility. The nature of this inflexibility stems from numerical complexity and a lack of connectivity to the underlying thermodynamic phenomena. The subject model defines critical non-dimensional parameters, which will enable transcritical systems to continuously operate at minimum power consumption. A further objective of this work is to establish a computational framework for online control and optimization that is adaptable to any design, working fluid or operating criteria.

System Description and Problem Definition

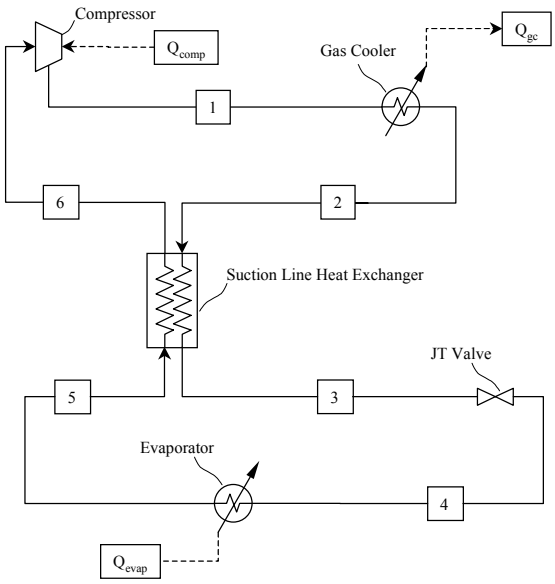

Figure 1. Transcritical Refrigeration Process Flow Diagram

Figure 1 depicts a commonly proposed embodiment of the transcritical refrigeration cycle. In reference to Figure 1, the working fluid is compressed to a supercritical pressure. The supercritical gas is subsequently cooled in a heat exchanger (gas cooler) typically utilizing an ambient utility (air/water) to absorb the gas-cooling load. The supercritical gas exits the gas cooler and is further cooled in a suction line heat exchanger (SLHX). The use of the SLHX represents the primary difference relative to a conventional vapor compression system (Rankine Cycle). The SLHX serves to mitigate flash losses in addition to reducing transcritical cycle sensitivity to variations in the supercritical gas cooler exit temperature. The supercritical stream exits the SLHX at a temperature near or below the critical temperature. The stream is then flashed to the evaporator pressure and vaporized by absorbing the external refrigeration load. The evaporator vapor is warmed in the SLHX and compressed as previously noted.

The primary intent of the following analysis is to identify non-dimensional parameters, which are suitable for dynamic determination of optimal high-side system pressure. A further, related objective is the identification of a minimum number of system observations required to compute the non-dimensional parameters.

The transcritical cycle's high operating pressure effectively mitigates the impact of pressure drop upon power consumption. For purposes of simplifying the following analysis, it has been assumed that there is a negligible pressure drop through the process heat exchangers ($P_1=P_2=P_3$, $P_4=P_5=P_6$). Considering the evaporator operation, a saturated vapor exit condition has been assumed. Although some superheating is unavoidable, liquid vaporization serves to absorb the bulk of evaporator load. The exit temperatures of the evaporator and gas cooler are assumed constant. These quantities represent inputs to the following analysis.

RESULTS AND DISCUSSION

The power consumed by a single, adiabatic compression stage is shown by Equation 1. In Equation 1, b is a constant possessing units of energy divided by mass and temperature. In order to establish the governing non-dimensional parameters, adiabatic compressor efficiency (η) is initially assumed constant.

$$Q_{comp} = \frac{bmT_6}{\gamma\eta}\left\{\left[\frac{P_3}{P_5}\right]^{\gamma} - 1\right\} \text{ where } \gamma = \frac{k\text{-}1}{k} \text{ and } k = {C_p}\big/{C_v} \tag{1}$$

Expression of refrigeration efficiency results from the relation of input power (Q_{comp}) to refrigeration effect or the energy absorbed by the evaporator (Q_{evap}). The energy absorbed within the evaporator is expressed as the product of the liquid mass flow (m) and the latent heat of vaporization (ΔH_{lv}) as shown in Equation 2.

$$Q_{evap} = x\ m\ \Delta H_{1v} \tag{2}$$

The liquid mass fraction (x) shown in Equation 2 is related to the enthalpies at points 4 and 5 (h_4, h_5). Isenthalpic expansion across the cold end JT valve dictates that $h_3=h_4$. Liquid mass fraction is computed by application of an enthalpy-lever rule. Substitution of this result into Equation 2 results in a Equation 3 which is simply the product of working fluid mass flow and enthalpy change across the evaporator.

$$Q_{evap} = \frac{(h_5 - h_3)}{\Delta H_{1v}}\ m\ \Delta H_{1v} = m\ (h_5 - h_3) \tag{3}$$

The common metric of refrigeration efficiency is the Coefficient of Performance (COP) which is the ratio of evaporator load to compressor power. For this analysis the inverse of the COP (f) is used to express efficiency. Equation 4 is the result of substituting Equation 3 into Equation 1.

$$f = {1}\big/{COP} = \frac{Q_{comp}}{Q_{evap}} = \frac{bT_6}{\gamma\eta\ (h_5 - h_3)}\left[\left(\frac{P_3}{P_5}\right)^{\gamma} - 1\right] \tag{4}$$

Equation 4 is naturally independent of mass flow (m). From calculus, differentiation and subsequent solution for the roots determine the optimum of any continuous function. For the process of Figure 1, differentiation of Equation 4 with respect to condenser/high side pressure will define the optimal condition Equation 5 (where $P_1=P_3$ as previously noted). With compressor efficiency (η) constant, application of Equation 4 to the optimality condition results in Equation 6.

$$\left[\frac{\partial f}{\partial P}\right]_3 = 0 \tag{5}$$

$$\frac{\partial f}{\partial P_3} = \left(\frac{1}{P_5}\right)\left(\frac{P_3}{P_5}\right)^{\gamma-1}(h_5 - h_3) + \left[\left(\frac{P_3}{P_5}\right)^{\gamma} - 1\right]\frac{1}{\gamma}\left\{\frac{\partial h_3}{\partial P_3} + \frac{(h_5 - h_3)}{T_6}\frac{\partial T_6}{\partial P_3}\right\} = 0 \tag{6}$$

Inspection of Equation 6 indicates that the derivatives of h_3 and T_6 with respect to pressure P_3 are required. Further reduction of this equation requires additional definition of these quantities. For low-pressure gases, enthalpy is not a function of pressure. However, at supercritical conditions, the pressure functionality of enthalpy must be accounted for in Equation 6. As a consequence, real gas properties must be utilized to satisfy Equation 6. Equation 7 displays the complete enthalpy relation for a real gas.

$$h = h_o^{ig} + Cp_{mh}^{ig}\ \left(T - T_o\right)\ +\ h^r\ ;\ \text{where}\ \ h^r\ = -T^2R\int_o^P\left(\frac{\partial Z}{\partial T}\right)_P\ \frac{dP}{P} \tag{7}$$

The only pressure dependent term in Equation 7 is the residual enthalpy, h^r. Differentiation of Equation 7 with respect to pressure yields Equation 8, which is subsequently into Equation 6. Equation 8 contains the temperature derivative of compressibility (Z). By definition, compressibility is a function of PVT information only (Z=PV/RT). Compressibility represents the deviation from the ideal gas state resulting from the effect of inter-molecular interaction.

$$\left[\frac{\partial h}{\partial P}\right]_3 = -\ \frac{RT_3^2}{P_3}\ \left(\frac{\partial Z}{\partial T}\right)_3 \tag{8}$$

Inspection of Equation 6 further indicates the need to define $\partial T_6/\partial P_3$. Developing such a quantity requires a relationship between T_6 and T_3. Since the steady state mass flow (m) through both sides of the SLHX is the same, T_6 and T_3 are related to energy balance. Alternatively, exchanger area and heat transfer correlation can be used to develop a relation between T_6 and T_3. This relationship is shown in Equation 9, where subscripts l and h refer to the average mass heat capacity at the low and high-pressure sides of the SLHX, respectively.

$$Cp_l\ \left(T_6\ -T_5\right) = Cp_h\ \left(T_2\ -\ T_3\right) \tag{9}$$

Equation 9 is rearranged and differentiation with respect to high side pressure (P_3). Since evaporation temperature (T_5), gas cooler and outlet temperature (T_2) have been assumed constants/inputs to this analysis; they are eliminated by subsequent differentiation. Assuming that Cp_h and Cp_l represent weighted average heat capacities, they are also treated as constants. Equation 10 is the differentiated form of Equation 9, which is substituted into Equation 6.

$$\frac{\partial T_6}{\partial P_3} = -\left[\frac{Cp_h}{Cp_l}\right]\left[\frac{\partial T}{\partial P}\right]_3 \tag{10}$$

Like enthalpy, the $\partial T_6/\partial P_3$ derivative can be related to real gas properties through compressibility (Z). Through chain rule and differentiation, $\partial T/\partial P$ for any real fluid is expressible in terms of compressibility (Equation 11).

$$\frac{\partial T}{\partial P} = \frac{T}{P}\ -\ \frac{T}{Z}\ \frac{\partial Z}{\partial P} \tag{11}$$

Substitution of Equation 11 into Equation 10 and hence into Equation 6 enables both derivatives contained within Equation 6 to be cast in terms of compressibility. After substitution, Equation 6 is rearranged and common terms collected. By introducing the non-dimensional pressure ratio (P_r) as the independent variable, two non-dimensional terms are produced. These non-dimensional parameters are arbitrarily referenced as Φ and Ψ. Equation 12 is the non-dimensional form of Equation 6.

$$\begin{gathered} P_r^\gamma\ -\ \left[P_r^\gamma - 1\right]\ \left(\Phi\ +\ \Psi\right) = 0 \quad \text{where; } P_r = P_3/P_5; \\ \Phi = \frac{T_3^2}{\left(h_5\ -\ h_3\right)}\frac{R}{\gamma}\ \left(\frac{\partial Z}{\partial T}\right)_3;\ \ \Psi = \frac{T_3}{\gamma T_6}\ \left[\frac{Cp_h}{Cp_l}\right]\left(1\ -\ \left(\frac{\partial \ln Z}{\partial \ln P}\right)_3\right) \end{gathered} \tag{12}$$

Determining the root(s) of Equation 12 requires knowledge of the compressibility derivatives contained in Φ and Ψ. Compressibility is typically defined from any number of sources, including actual PVT data, correlation of such data or an equation of state.

Closer examination of non-dimensional parameter Φ indicates that if T_3 is known, the only other quantity required for evaluation is the enthalpy difference across the evaporator. Since enthalpy is a thermodynamic construct, it must

be computed or inferred from quantities that are observed or specified. In actual system operation, Φ can be used as a means for introducing the desired-specified evaporator load. Alternatively, evaluation of the enthalpy difference across the evaporator may be accomplished by measuring the existing evaporator load. As an example, cooling a known flow of air to a desired temperature allows direct calculation of the enthalpy difference. Dividing the known or desired load by the working fluid mass flow (m) provides the enthalpy difference required to evaluate Φ. In addition to the air inlet and outlet temperatures and flow, the mass flow of refrigerant must also be known. Equation 13 illustrates a possible calculation route.

$$h_5 - h_3 = \frac{Q_{evap}}{m} = \left(\frac{m_{air}}{m}\right) \bar{C}p_{air} \quad \Delta T_{air} \tag{13}$$

Other than the logarithmic compressibility derivative, evaluation of non-dimensional parameter Ψ requires additional knowledge of SLHX operation/exit temperatures. If the ratio of SLHX heat capacity is known, at least one other SLHX exit temperature is required (e.g. T_6). Alternatively, rearrangement of Equation 9 and subsequent substitution into Ψ results in Equation 14. Inspection of Equation 14 indicates that measurement of the four inlet/exit SLHX temperatures (T_2, T_3, T_5, T_6) is used to compute non-dimensional parameter Ψ. Alternative embodiments of Equation 14 are possible given the definition of the SLHX heat transfer area and performance.

$$\Psi = \frac{\left(1 - T_5/T_6\right)}{\left(1 - T_2/T_3\right)} \frac{1}{\gamma} \left[\left(\frac{\partial \ln Z}{\partial \ln P}\right)_3 - 1\right] \tag{14}$$

Assuming the compressibility derivatives are known, several additional system observations are required for dynamic transcritical cycle optimization. From Equation 12, these observations include the existing compression ratio as well as the evaporator and gas cooler outlet temperatures. In addition, at least one other SLHX exit temperature is required. Evaluation of Φ will likely require knowledge of system mass flow.

CO_2 Compressibility

In order to illustrate the impact of real gas properties upon the subject model, the compressibility derivatives contained within non-dimensional parameters (Φ and Ψ) were evaluated[7] for CO_2. The results of this analysis are shown graphically in Figures 2 and 3. In general, the temperature differential (Figure 2) increases with increasing temperature and decreases with increasing pressure. Above the critical temperature, substantial non-linear behavior is apparent. In contrast, the logarithmic compressibility differential (Figure 3) decreases with increasing temperature and increases with increasing pressure. At lower temperatures, all curves of varying pressure become asymptotic and essentially linear.

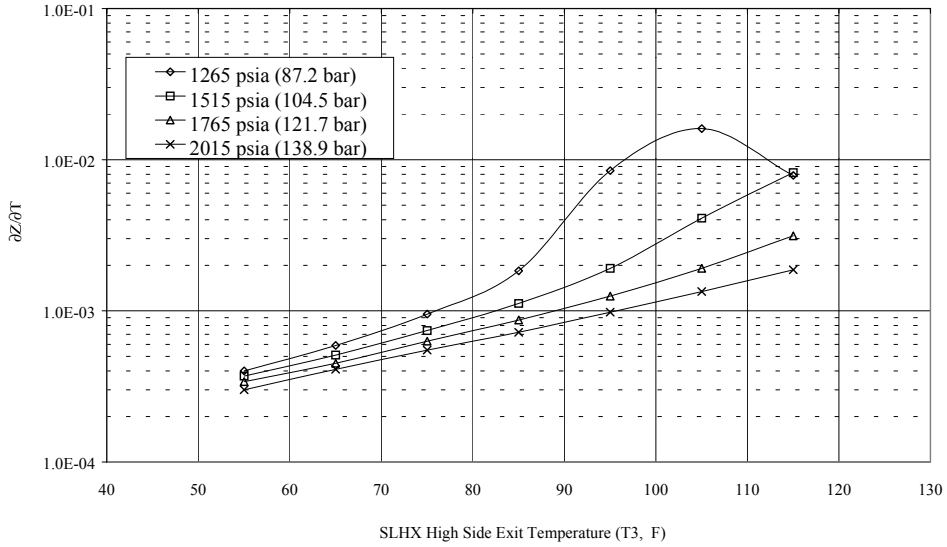

Figure 2. CO_2 Compressibility Differential w/to Temperature

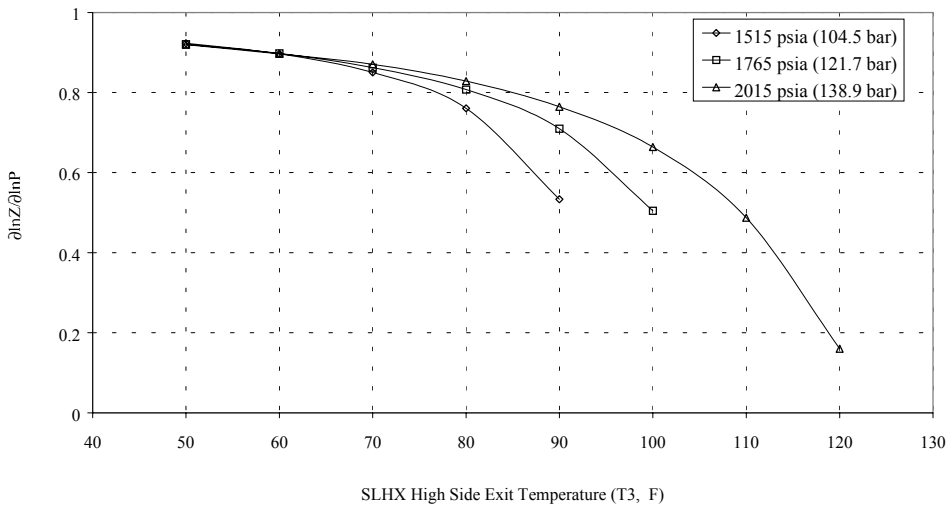

Figure 3. CO_2 Logarithmic Compressibility Differential w/to Pressure

Initial consideration of Figures 2 and 3 and the conditions relevant to transcritical CO_2 cycle operation (T_3, 68 – 104 F (20-40 C) , P_3, 1160 – 2030 psia (80-140 bar)), imply that dynamic calculation of the subject differentials is essential. For a control system, calculation of such differentials would clearly be cumbersome. However, detailed evaluation of the locus of optima and the associated differentials indicates that such a procedure is unnecessary. Figure 4 depicts a family of curves representing maximum COP at varying gas cooler exit temperatures (constant evaporator temperature, 40 F (4.6 C)). At the maximum COP for each curve, the associated differentials are virtually constant. The compressibility differentials are therefore a characteristic of the optima and can be treated as such in model Equation 12.

In reference to Figure 4, the open symbols represent points where the actual/observed P_r and the computed/optimal P_r (from Equation 12) are equivalent. The open triangles represent points generated using a rigorous computation of the compressibility differentials (the values of which are shown in the Figure 4). The open squares represent points where the compressibility differentials were held constant across the entire range. Comparison of each locus of optima indicates little variation in the observed COP between each approach. Assuming constant differentials results in a power penalty of less than 1% across the entire range considered. It can be accurately concluded that dynamic knowledge of compressibility differentials is unnecessary for model implementation.

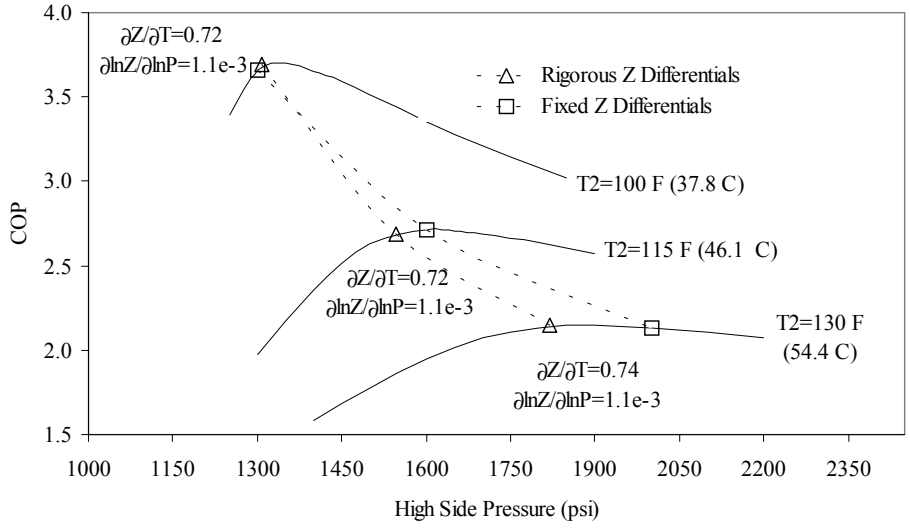

Figure 4. Non-Dimensional Model Performance for Figure 1 with CO_2 and Constant Compressor Efficiency

The implications of the above result are considerable. First, the fact that the compressibility differentials are essentially constant indicates that the transcritical system can be optimized without prior knowledge of supercritical enthalpy functionality. Furthermore, given any system design or working fluid, the differentials and other physical constants can be lumped into system tuning parameters. Since the functionality of Equation 12 is based upon thermodynamic fundamentals, confidence in extrapolation is substantially increased.

Non-Constant Compressor Efficiency

The previous analysis is based upon constant compressor efficiency. Actual system operation will be characterized by non-constant compressor efficiency. Variation in pressure ratio often leads to substantial changes in adiabatic compression efficiency. Equation 12 can be easily extended to account for actual compressor performance.

If adiabatic compression efficiency is known to be a marginal function of pressure ratio it can be treated as a pseudo-constant. Inspection of Equation 1 and Equation 12 indicates that simple algebraic rearrangement of terms leads to the elimination of Pr. Equation 15 is Equation 12 recast in a form which provides an optimal/target compressor energy consumption from knowledge of the subject non-dimensional parameters and associated system observations/temperatures.

$$\frac{Q_{comp}}{\beta} = \frac{1}{(\Phi + \Psi - 1)} \quad \text{where;} \quad \beta = \frac{bmT_6}{\gamma\eta} \tag{15}$$

If efficiency is a strong function of pressure ratio its effect must be integrated into the non-dimensional parameter development. It is known that the variability of compressor efficiency is often a linear power law of compression ratio. Equation 16 relates adiabatic efficiency to compression ratio. The functionality is arbitrary. However, use of the adiabatic compression power constant γ greatly simplifies subsequent analytic reduction of the model equations.

$$\eta = a_1 \; P_r^{\gamma} \; + \; a_2 \tag{16}$$

Equation 16 and its derivative are introduced into the differentiated form of Equation 4. Subsequent reduction is omitted for brevity. The results of this analysis indicate that the previous non-dimensional parameters (Φ and ψ) definition remains unchanged. Formulation of Equation 16 using $P_r{}^{\gamma}$ as a basis enables the governing equation to be formatted into a quadratic equation whose roots can be solved for explicitly.

$$\Theta y^2 \; - \; \left(A\left(1 \; - \; \Theta\right) + \quad \left(1 \; + \; \Theta\right)\right) \; y \; - \; A\Theta = 0 \quad \text{where;} \quad \Theta = \Phi + \Psi; \quad y = P_r^{\gamma}; \quad A = {a_2}/{a_1} \tag{17}$$

The accuracy of Equation 17 was investigated. Representative values for Equation 16 (a_1 and a_2) were regressed from the published performance a semi-hermetic CO_2 compressor[8]. Figure 5 provides a comparison of model results relative to the actual COP observed with non-constant compressor efficiency. The compressibility derivatives were held constant across the range. Inspection of Figure 5 indicates that the introduction of non-constant compressor efficiency does not compromise model integrity. Furthermore, the maximum power penalty incurred by use of the model did not exceed 1% across the range shown (relative to the known maximum COP).

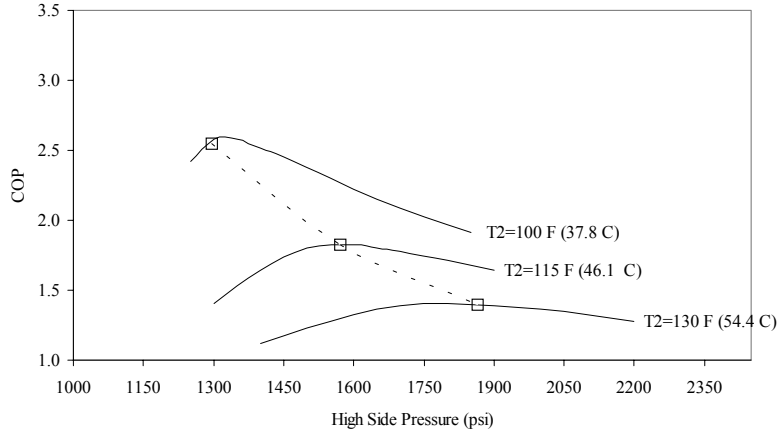

Figure 5. Model Performance for Figure 1 with CO_2 and Non-Constant Compressor Efficiency

CONCLUSIONS

In summary, the subject phenomena-based model allows for continuous prediction of optimal high side operating pressure of transcritical cycles. The model is independent of working fluid. Two non-dimensional parameters were determined analytically. Although the use of real gas properties form the basis of this derivation, dynamic knowledge of real gas properties is unnecessary. Model development has led to the conclusion that several system observations are required to drive the transcritical cycle to minimum power consumption. These observations are the outlet temperatures of the gas cooler and evaporator, the system mass flow, evaporator load, existing compression ratio and at least one SLHX outlet temperature. An alternative formulation of the model is provided that accounts for compressor efficiency and utilizes compressor power consumption in lieu of system pressure ratio.

The model provides a number of practical benefits to transcritical cycle operation. The primary advantage is the establishment of a fundamental methodology for dynamic/continuous process optimization of the transcritical cycle. For instance, Equation 15 can be used to project optimal power consumption through observation of several system variables. Compressor discharge pressure is subsequently adjusted to minimize the difference between the projected optimal power consumption and that actually observed from the compressor. If a formulation similar to Equation 17 is used, the compressor discharge pressure can be directed to an optimal condition by minimizing the difference between the observed high side pressure and that value computed by the model equation.

Unlike prior empirical approaches, the subject model adapts to changes in equipment or working fluid. For instance, if temperature is used to determine non-dimensional parameter Φ, the model dynamically accommodates exchanger fouling or increased system pressure drop. The non-dimensional parameters are independent of compressor performance. Although the intent of this development was a displacement of empirical models, the governing non-dimensional parameters can be recast into any number of formats and/or empirical correlation(s). The fundamental nature of the model allows for direct introduction of system setpoints such as ambient conditions, evaporator temperature or desired evaporator load. These features combine to provide a substantial improvement in the understanding of transcritical cycle operation.

REFERENCES

1. Lorentzen, G., “The Use of Natural Refrigerants,” Proceedings of IIR Conference, New Applications of Natural Working Fluids in Refrigeration and Air Conditioning, pp. 23-36, 5/1993
2. Lorentzen, G., Pettersen, J., Bang, R., “Method and Device for High Side Pressure Regulation in Transcritical Vapor Compression Cycle,” US Patent 5245836, 9/21/1993
3. Lorentzen, G., Pettersen, J., “Transcritical Vapor Compression Cycle Device with a Variable High Side Volume Element,” US Patent 5497631, 3/12/1996
4. Liao, S.M., Zhao, T.S., Jakobsen, A., “A Correlation of Optimal Heat Rejection Pressures in Transcritical Carbon Dioxide Cycles,” Applied Thermal Engineering, No. 20, pp. 831-841, 2000
5. McEnaney, R.P., Hrnjak, P.S., “Control Strategies for Transcritical R744 Systems,” SAE Paper Number 2000-01-1272
6. Vaisman, I., “Thermodynamic Analysis of Carbon Dioxide Cycles,” 4th IIR Gustav Lorentzen Conference on Natural Working Fluids, pp. 25-32, 7/2000
7. NIST Standard Reference Database 12, 1992-NBS Technical Note 1097 1986
8. Neksa, P., et.al., “Development of Semi-Hermetic CO2 Compressor,” 20th International Congress of Refrigeration, Sydney 1999